

Dismountable steel tensegrity grids as alternate roof structures

Ramakanta Panigrahi, Ashok Gupta and Suresh Bhalla*

Civil Engineering Department, IIT Delhi, India

(Received November 30, 2007 Accepted December 24, 2008)

Abstract. This paper reviews the concept of tensegrity structures and proposes a new type of dismountable steel tensegrity grids for possible deployment as light-weight roof structures. It covers the fabrication of the prototype structures followed by their instrumentation, destructive testing and numerical analysis. First, a single module, measuring 1 m × 1 m in size, is fabricated based on half-cuboctahedron configuration using galvanised iron (GI) pipes as struts and high tensile stranded cables as tensile elements. Detailed instrumentation of the structure is carried out right at the fabrication stage. The structure is thereafter subjected to destructive test during which the strain and the displacement responses are carefully monitored. The structure is modelled and analyzed using finite element method (FEM) and the model generated is updated with the experimental results. The investigations are then extended to a 2 × 2 grid, measuring 2 m × 2 m in size, fabricated uniquely by the cohesive integration of four single tensegrity modules. After updating and validating on the 2 × 2 grid, the finite element model is extended to a 8 × 8 grid (consisting of 64 units and measuring 8 m × 8 m) whose behaviour is studied in detail for various load combinations expected to act on the structure. The results demonstrate that the proposed tensegrity grid structures are not only dismountable but also exhibit satisfactory behaviour from strength and serviceability point of view.

Keywords: tensegrity; dismountable; finite element method (FEM); strain; monitoring.

1. Introduction

The term ‘tensegrity’, coined by Fuller (1962) as a contraction of the two words, ‘tension’ and ‘integrity’, is a novel concept in the field of structural engineering. A tensegrity structure typically consists of a set of discontinuous compression members, tied together by a set of continuous tensile members. Since tensile elements impart a lightweight appearance, Fuller characterized these systems as “small islands of compression in a sea of tension”. In contrast to the conventional cable structures, tensile forces in the tensegrity structures are controlled by their inner self-stress states only. Hence, these structures are self-supporting, without warranting expensive anchorages. Wang and Li (2003) described the tensegrity systems as freestanding pin-jointed cable networks, in which a connected system of cables are stressed against a disconnected system of struts. Similarly, Snelson (2004) described the tensegrity systems as closed structural systems composed of a set of three or more elongate compression struts within a network of tension tendons, the combined parts mutually supported such that the struts do not touch one another, but press outwardly against nodal points in the tension network to form a firm, triangulated and prestressed

* Assistant Professor, Corresponding Author, Email: sbhalla@civil.iitd.ac.in

system. Fig. 1 (a) shows a simplex type tensegrity structure consisting of three compression and nine tensile elements. Another simple tensegrity system, called half cuboctahedron, is shown in Fig. 1(b). It consists of four struts and twelve cables such that the top square is inscribed in the bottom one, thereby making the nodes the apices of a half-cuboctahedron.

Although the concept of tensegrity structures evolved in 1960s, it was in the 1990s that they generated major research interest. Hanaor (1993) fabricated a three-unit flat tensegrity model consisting of three simple 'T' prisms using telescopic tubes with O-ring seals and deployed it by means of air pressure. You and Pellegrino (1997) proposed a tensegrity based support structure for a large mesh reflector, consisting of a cable-stiffened pantographic ring which in turn pretensioned the cable network. From the point of view of structural mechanics, the most prominent characteristic of the tensegrity structures is that they exhibit large deformations when subjected to loads, thereby necessitating the inclusion of geometric non-linearity in their structural analysis (Gantes 1997, Kebiche, *et al.* 1999). Stern (1999) carried out the generalized non-linear static analysis of 'n-strut' tensegrity systems and derived design equations for self-deployable systems. Quirant, *et al.* (2003) designed a tensegrity based roof system capable of supporting loads up to 18kg/m^2 based on half-cuboctahedron configuration as per the Euro codes. Tibert and Pellegrino (2002) proposed a deployable tensegrity prism structure using two identical cable nets (front and rear) interconnected by tension ties, with a reflecting mesh attached to the front net. A small-scale physical model was fabricated to demonstrate the proposed concept. Fest, *et al.* (2004) reported the fabrication and testing of a full-scale prototype of an adjustable tensegrity structure. The test results indicated linear behaviour under vertical loads on a single joint but nonlinear behaviour under vertical loads applied to several joints. Tibert and Pellegrino (2003) presented the design of a deployable tensegrity mast, covering form finding, structural analysis, manufacturing and deployment. The deployment of the mast was achieved using self-locking hinges and cables forming the outer envelope of the mast through two-dimensional weaving. Sultan and Skeleton (2003) developed a new deployment strategy for tensegrity structures based on the assumption that the structure yields an initial equilibrium configuration with all tendons in tension. The control variables were considered as the length of the struts or the lengths of the tendons or

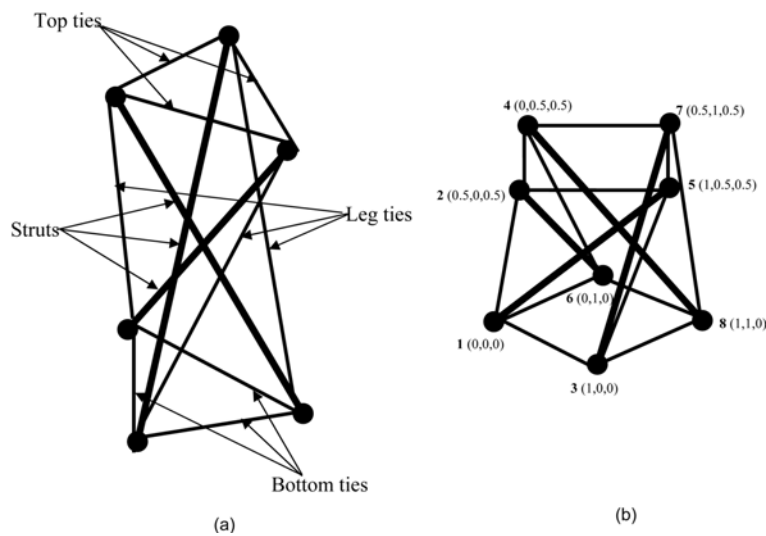


Fig. 1 (a) A Simplex type tensegrity structure, (b) Half cuboctahedron module

a combination of the both. They found that the control variables take values only in the set of the equilibrium manifold. Vu, *et al.* (2005, 2006) introduced tensegrity systems consisting of detachable elements so as to decouple the structural design from kinematic requirements. Fu (2005) studied the structural behavior of tensegrity domes and proposed a design methodology by summarizing the results obtained through non-linear analysis. Zhang and Ohsaki (2006) derived the stability conditions for tensegrity structures based on positive definiteness of the tangent stiffness matrix (i.e. sum of the linear and geometrical stiffness matrices).

The literature review suggests that the vast majority of research on tensegrity structures focused on theoretical and design aspects. Only a handful of experimental research works have been reported covering their fabrication, instrumentation and destructive testing. Majority of the experimental studies reported in the literature were restricted to small models only. The full potential of the tensegrity structures as alternate roofs for modern structural systems has not been studied and practically utilized. In the research reported in this paper, two tensegrity prototypes - a single module and a 2×2 grid, have been fabricated based on half-cuboctohedron configuration and subjected to destructive tests. The grid was fabricated as a cohesive unit by joining four single units along the base cables rather than at the nodes. The experimental investigations consisted of material characterization, fabrication, instrumentation and comprehensive monitoring using electrical strain gauge (ESGs) and linear variable differential transducers (LVDTs). A finite model was developed, updated with experimental data and validated with the experimental results of the 2×2 grid. It was then extended to 8×8 grid which was analyzed for various load combinations to explore the possibility of covering large spans. The following sections cover each of these aspects in detail.

2. Material characterization

Tensegrity structures consist of soft members, the cables, and hard members, the struts. It is essential to determine the material properties such as the Young's modulus and the strength of both the member types. In this study, galvanized iron (GI) pipes of medium type, conforming to the Indian Standards (IS 1239-I 1990), were employed as compression members. The average internal and external diameters of the pipes were determined as 15.900 and 21.375 mm respectively by measurement, resulting in a cross sectional area of 160.284 mm². From tension test, the Young's modulus of elasticity of the pipes was determined as 2.05×10^5 N/mm² and the ultimate stress as 410 N/mm². The cables used for the reticulated network were made of 0.27 mm galvanized high carbon steel wires conforming to the Indian Standard IS 1835 (1976). Each cable consisted of six strands with nineteen wires in each in accordance with IS 3459 (1977), resulting in a total cross-sectional area of 6.53mm². The Young's modulus of the stranded wire was experimentally determined as 0.954×10^5 N/mm². The yield stress and 0.2% proof stress were experimentally determined as 1421.335 N/mm² and 1119.575 N/mm² respectively. It should be noted that the cables possess much higher strength, several times in magnitude, as compared to the struts. A critical parameter in the design of the tensegrity structures is the rigidity ratio, defined as

$$r = \frac{E_s A_s}{E_c A_c} \quad (1)$$

where E_s and E_c respectively denote the Young's modulus of elasticity of the struts and cables and A_s and A_c their areas of cross section. With the presently employed strut-cable combination, this ratio works out to be 52.74.

3. Fabrication, testing and modelling of single module

Fig. 2 shows the fabrication of a single tensegrity module using GI pipes and stranded cables, at various stages during the erection. The bottom cables were 1 m, the top and the side cables 0.707 m and the struts 1.224 m in length, measured centre to centre of joints. At each joint, 12 mm eyebolts were used for connecting the cables to the strut member. By providing a turnbuckle in one of the top cables, as shown in Fig. 2(b), the structure was rendered dismantlable, i.e. it can be conveniently erected and thereafter dismantled and packaged after use. During erection, the turnbuckle needs to be kept loosened initially. After fitting the struts in required position, the length of the top cable can be adjusted by tightening the turnbuckle. Once the length of adjustable top cables became equal to 0.707 m, the structure attains self stressed equilibrium. Hence, the struts and the cables carry stresses even in the unloaded condition. To determine the forces in the struts and the cables, ESGs of 5mm gauge length, manufactured by TML (2006) and conforming to product FLA-5-11 were surface bonded on the struts. Four ESGs were bonded

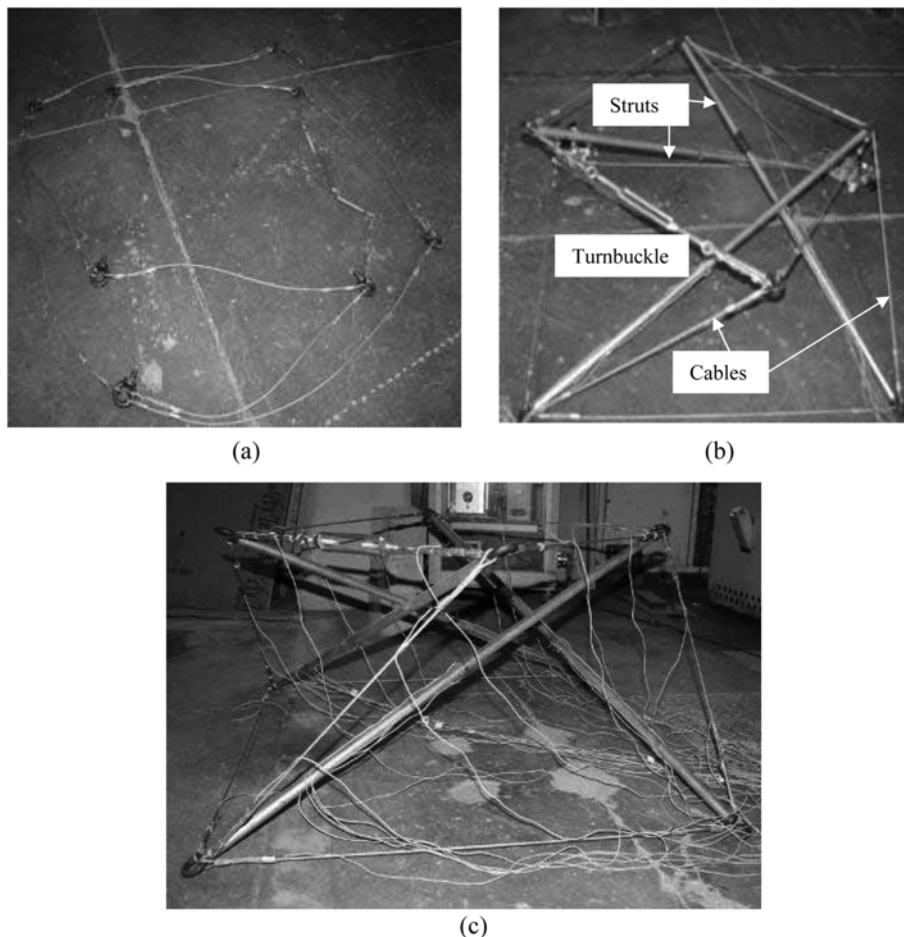


Fig. 2 Different stages of erection of single tensegrity module
(a) Laying cables (b) Fitting struts and erecting (c) Ready for test

on the GI pipes parallel to the axis and uniformly spaced along the circumference. Average axial strain was measured using these ESGs so as to eliminate possible bending effects (Batten, *et al.* 1999). All the ESGs were instrumented before erection (tightening by turnbuckle) so that the initial prestresses could be determined accurately. In addition, two LVDTs were fitted below two top nodes so as to measure the deflection in vertical direction. The prestress force in the struts was measured to be 2.58 kN on an average from the measured strain data.

The structure was tested quasi-statically by gradually increasing the vertical loads applied by means of an iron plate and concrete cubes, as illustrated in Fig. 3. The structure began to undergo large deflections, at around a load of 2.45 kN, and finally collapsed at 3.25 kN, resulting from the buckling of a strut. The failure pattern is shown in Fig. 4. Considering ideal conditions at the ends i.e. no rotational restraints, the allowable compression load of this member was computed as 5.15 kN. However, the strut actually withstood a much higher force of 12.77 kN. It can therefore be concluded that actual condition at the ends must be that of partial fixity, which increased the load carrying capacity of the struts by reducing the slenderness ratio. By trials, an effective length ratio of 0.7 was found to predict the load carrying capacity in agreement with the experiment.

The structure tested above was modelled using FEM. The detailed procedure for large deflection analysis of prestressed cable networks using matrix displacement approach has been described by Argyris and Scharpf (1972). Presently, the finite element analysis was performed using ANSYS 9 (2004). All the cable and the strut elements were modelled as 3D spar elements with three degrees of freedom in translation at each node. The material was assumed as linearly elastic and isotropic. Fig. 5 shows the model generated using the preprocessor of ANSYS 9. All the bottom nodes i.e. 1, 3, 6 and 8, were restrained against translation in the vertical direction only, and initially allowed to undergo horizontal displacement since during the experiment, no external horizontal restraint was applied other than natural friction. The values of the Young's moduli of the strut and the cable elements obtained experimentally were used. Similarly, the prestress forces in the self stressed equilibrium configuration obtained

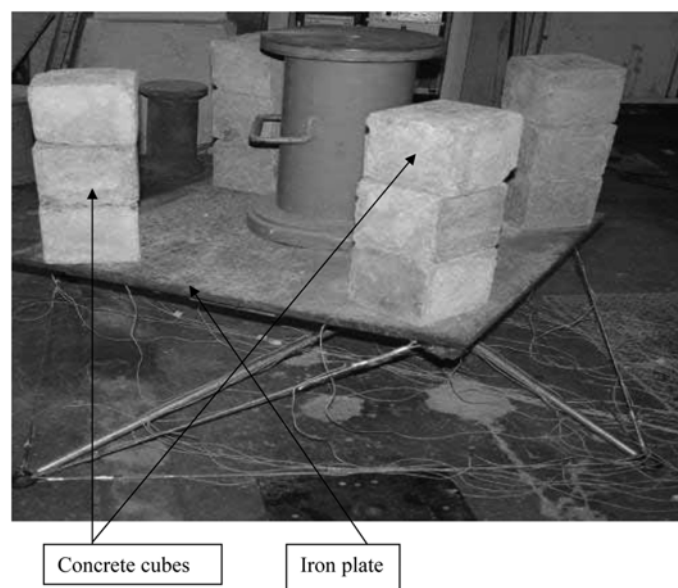


Fig. 3 Destructive testing of single tensegrity module

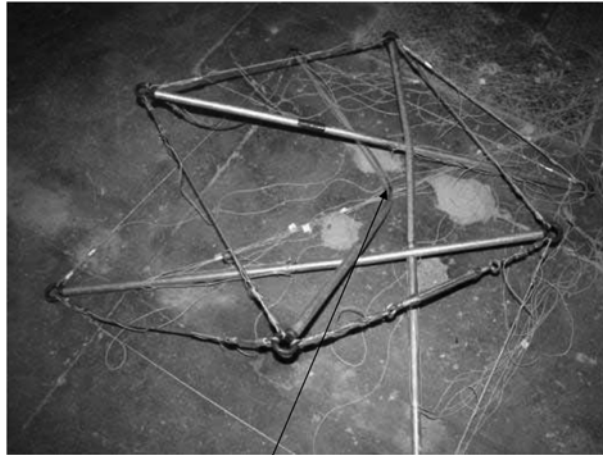


Fig. 4 Failure pattern of single module

experimentally through strain measurement in the struts were used for analysis. The prestress forces in the cables were worked out from the equations developed by Stern (1999) i.e.

$$aF_a = bF_b \tag{2}$$

and

$$\frac{F_t}{L_t} = \frac{F_s}{L_s} \tag{3}$$

where F_a is the force in the top cable, F_b in the bottom cable, F_t in the leg ties and F_s in the struts.

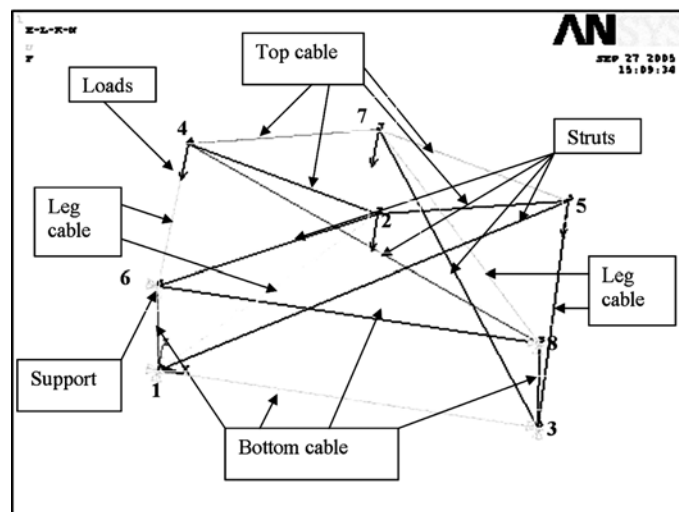


Fig. 5 Finite element model of single tensegrity module

Further, a is the length of top cable, b that of the bottom cable, L_t that of the leg tie and L_s that of the strut. Further, F_s and F_t can be expressed in terms of F_a and F_b as

$$F_s = \frac{2L_s}{b} F_a \sin\left(\frac{\pi}{n}\right) \quad (4)$$

and

$$F_t = \frac{2L_t}{b} F_a \sin\left(\frac{\pi}{n}\right) \quad (5)$$

By considering $a = 0.707\text{m}$, $b = 1.0\text{ m}$, $L_t = 0.707\text{ m}$ and $L_s = 1.224\text{ m}$ (for the half cuboctohedron configuration), the relations given by Eqs.(1) to (4) yield

$$F_a = F_t = 0.578F_s \quad (6)$$

and

$$F_b = 0.409F_s \quad (7)$$

F_a , F_t and F_s values determined from these equations corresponding to the measured strut force $F_s = 2.58\text{ kN}$ were considered in the finite element analysis. The model was simulated with the external loads applied on the structure (as in the experiment), distributed equally among all top nodes as concentrated loads. Fig. 6 compares the vertical deflections predicted by the FEM with the average deflections measured at the top nodes 4 and 7. It is observed that the FEM overestimates the deflection, the errors lying in the range of 10% to 22%. To minimize the discrepancy between the experimental and the FEM results, the FEM model was updated by trial (Panigrahi 2007). Best match was observed for the case of the finite element model with the translations locked in all the three directions at the bottom nodes 1, 3, 6, 8 (see Fig. 5). Fig. 7 shows the comparison of deflections for the updated model. This shows that the boundary conditions of the bottom nodes of the structure are closer to that of full fixity arising out of the friction forces from the floor surface acting on the four nodes. Further validation of the updated model is presented by Fig. 8, which shows a comparison of the measured average strut forces with those

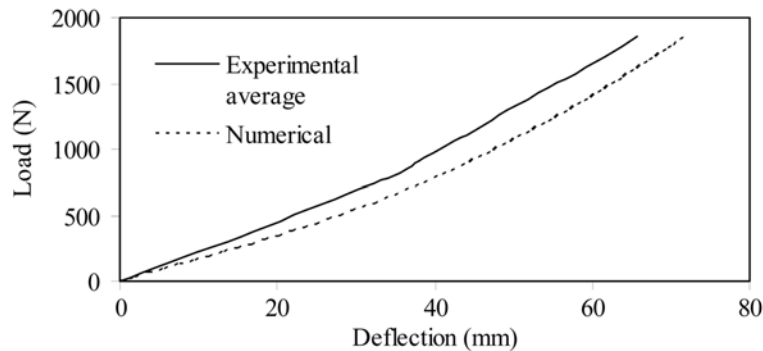


Fig. 6 Comparison of measured deflection with that predicted by FEM for single tensegrity module

predicted by the updated FEM, where good agreement can be observed between the two. The next section extends the fabrication, testing and analysis to a 2×2 grid structure.

4. Fabrication, testing and modelling of tensegrity grid

After successful fabrication of the single module, a dismantable 2×2 tensegrity grid (measuring 2×2 m in size) was fabricated by integrating four single tensegrity modules of the type described in the previous section. Fig. 9 shows a pictorial view of the fabricated prototype structure after erection, supported on four supports made of composite columns of 75 cm diameter and 1 m height. This grid is quite different in fabrication as compared to other similar tensegrity grids reported in the literature (eg. Hanaor 1993, Quirant, *et al.* 2003, Fest, *et al.* 2004), all of which were fabricated by joining the individual single units at the common nodes. In the new grid, on the other hand, the various subunits have been connected along the common bottom cables and the top nodes. As a result, the number of cables is reduced by four as compared to the conventional fabrication approach. In addition, the resulting grid is expected to be stiffer, since two or more struts are meeting at such joints.

Special joints were fabricated for achieving the complex connection of the struts and the cables. Fig.

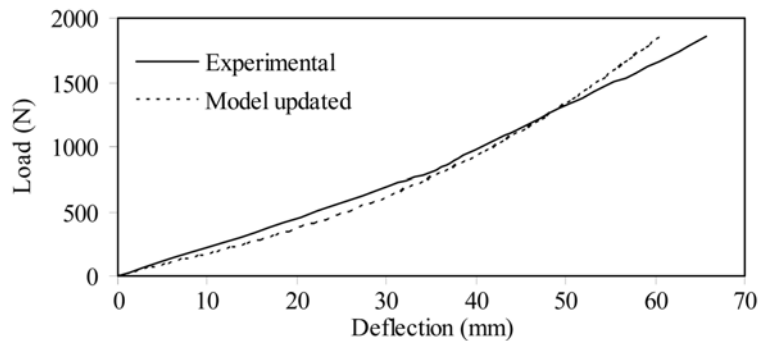


Fig. 7 Comparison of measured deflection with that predicted by FEM after updating for single tensegrity module

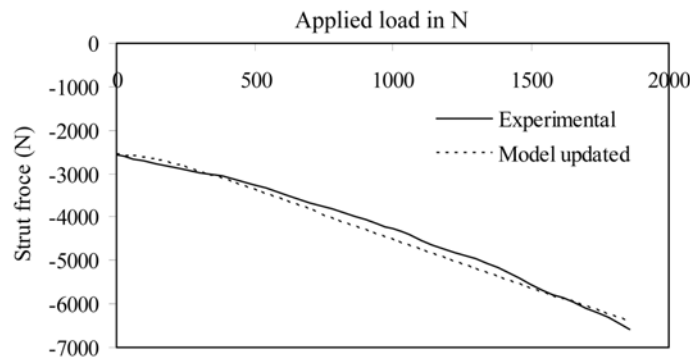


Fig. 8 Comparison of strut force between experiment and updated numerical model

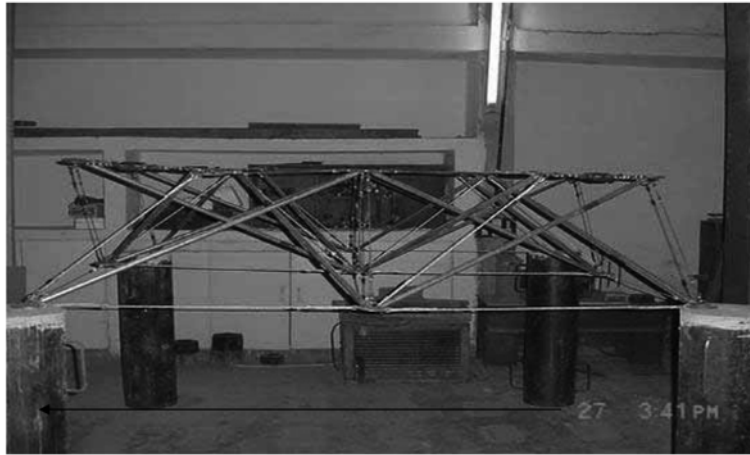


Fig. 9 Tensegrity prototype grid by integrating four single modules

10 shows a typical bottom joint of the structure to facilitate such a connection. A mild steel plate 10 cm in diameter and 5 mm in thickness was chosen as the base plate. For connecting the top and the bottom cables, holes were drilled in the plate at appropriate locations obtained from the geometry. For connecting the struts, 16 mm diameter mild steel rods of 80 mm length were welded on this plate at suitable positions with desired orientation. This was the most challenging task. In addition, mild steel hooks were welded for connecting the leg cables. All the cables were passed around the holes or the hooks (as applicable) and secured by hydraulic press.

All members of one unit (quarter) of the grid were instrumented with ESGs, four on each pipe (5 mm gauge length) and two on each cable (2 mm gauge length). One LVDT was placed under the central bottom node and the other was under a side bottom node. From strain measurements, the average prestress force in the struts was found to be 2.13 kN. The average prestress force in the top, bottom and tie cables was experimentally measured to be 0.79 kN, 1.19 kN and 1.27 kN respectively. Fig. 11 shows the finite element model of the structure, with the modelling carried out on the lines of the single module. All the element lengths, element types and the boundary conditions were kept the same. The grid was assumed to be



Fig. 10 Detail of central bottom joint

supported at the four outer nodes, which were restrained against movement in all the three directions, based on the experimental observations on the single module. The structure was loaded quasi-statically by placing iron weights on wooden plate resting on the top nodes using an electrically operated crane, simulating uniformly distributed load. All the strains and the deflections were continuously recorded. The structure finally failed at a total load of 6.19 kN resulting from the failure of the U-hook of one of the top joints, as shown in Fig. 12. As a result, the cable connecting nodes 11 and 12 underwent snap. In addition, joint 16 underwent large permanent deflection. However, there was no sign of any strut failure till this stage. Maximum cable force of 4 kN was observed at failure, which is thus the force the U-hook can withstand.

Fig. 13 shows the deflection measured at bottom node 3 (see Fig. 11b) of the tensegrity grid and compares it with that predicted by FEM. A very good agreement is observed between the two, with the maximum error being 6% only. Fig. 14 shows the variation of force in the strut connecting nodes 3 and 10 and Fig. 15 in the bottom inner cable connecting nodes 3 and 11, obtained experimentally as well as computed using FEM. Again, a very good agreement can be observed between the experimental and the numerical results. Thus, having validated the finite element model, it can be extended to analyze 8m span grid structures, as covered in the next section.

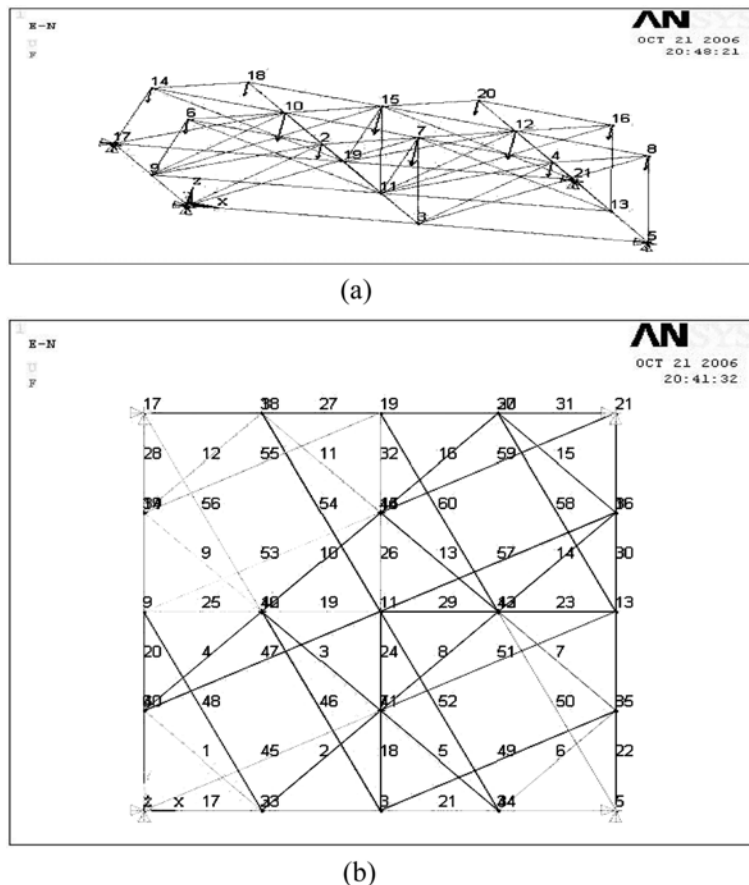


Fig. 11 Finite element model of 2×2 tensegrity grid structure (a) Perspective view (b) Top view

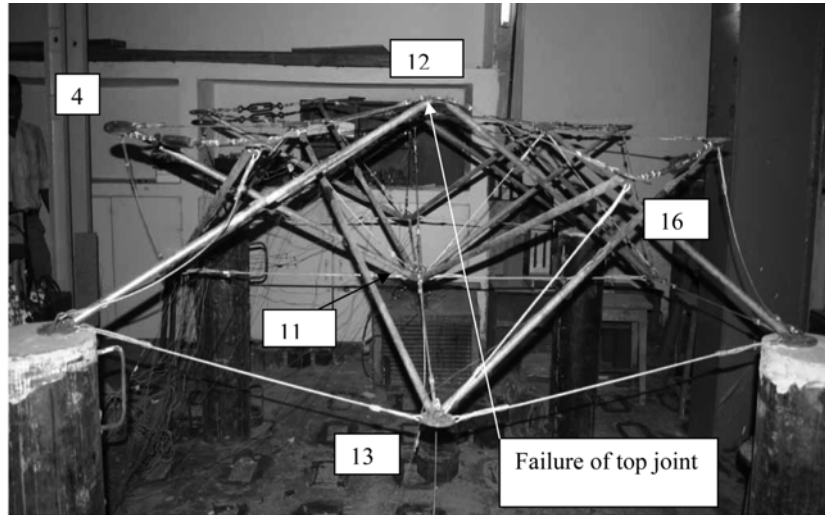


Fig. 12. Tensegrity grid structure after failure

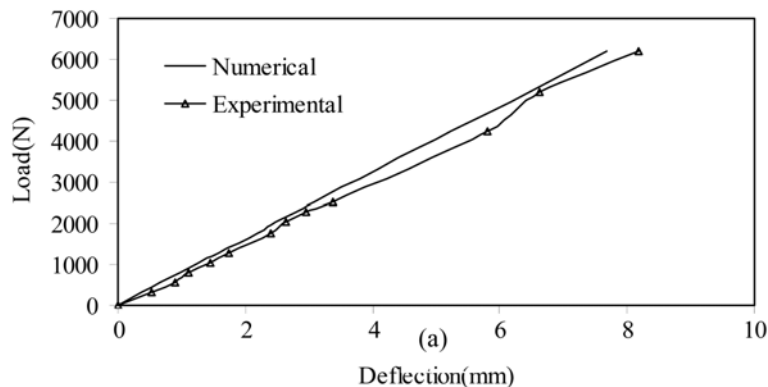


Fig. 13 Comparison of deflection at node 3 of tensegrity grid

5. Behaviour of large span tensegrity grids

The proposed structural system offers a ready-to-erect roof system that can be expanded when required in the field and also packaged after use. Hence, it is especially suitable for temporary structures. However, practical requirements might necessitate larger spans, of the order of 6 to 10m. In general, the FEM and the experimental results of both the deflections as well as the member forces match reasonably well with each other. Hence, in this study, an 8x8 tensegrity grid (measuring 8 × 8 m) was simulated using FEM and its behaviour studied under dead loads, imposed loads and wind loads.

Any roof system suitable for field deployment must satisfy both strength and serviceability criteria. From strength point of view, the load capacities of the struts, the cables and the joints should be adequate. The maximum allowable compressive force in the strut was worked out to be 8.97 kN as per IS 800 (1984), using the experimentally determined yield strength and considering an effective length coefficient of 0.7 in consistency with the observed experimental behaviour. Similarly, the allowable tensile force in

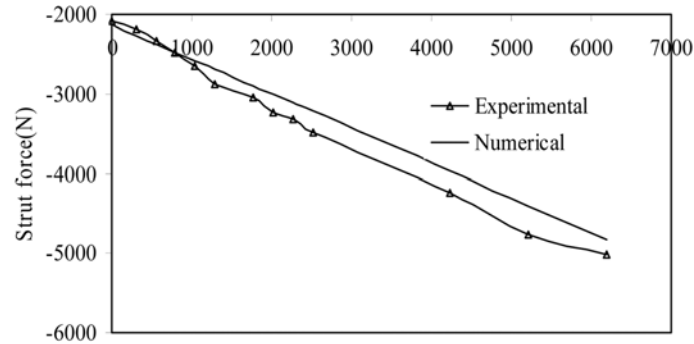


Fig. 14 Comparison of force in strut connecting nodes 3 and 10 of tensegrity grid

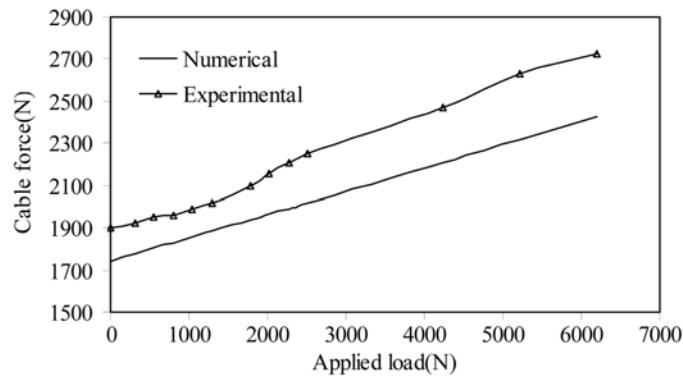


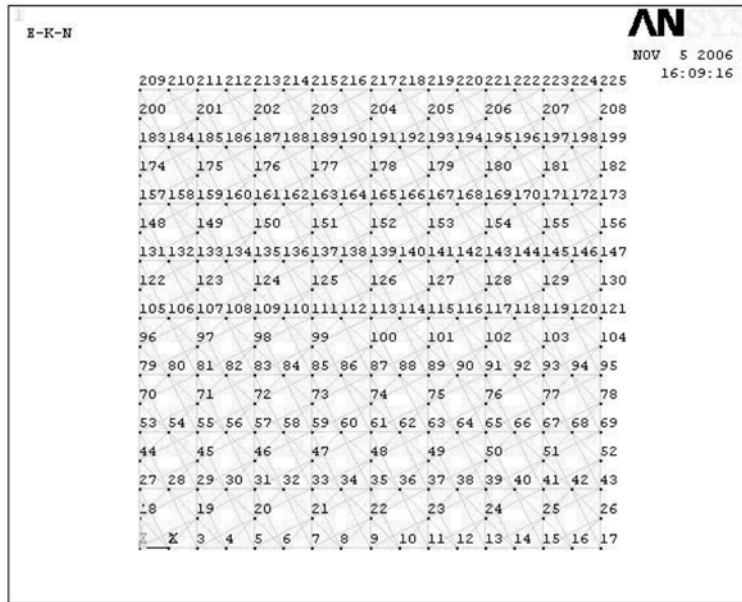
Fig. 15 Comparison of force in bottom cable connecting nodes 3 and 11 of tensegrity grid

the cables was computed to be 4.38 kN based on the experimentally determined yield stress of 1119.575 N/mm². However, considering the U-hooks of the joints, the cable would be able to withstand a force of 4 kN only as observed experimentally in the 2 × 2 grid. From serviceability point of view, the vertical deflection should not exceed span/ 325 (IS 800 1984), i.e. 24.6 mm.

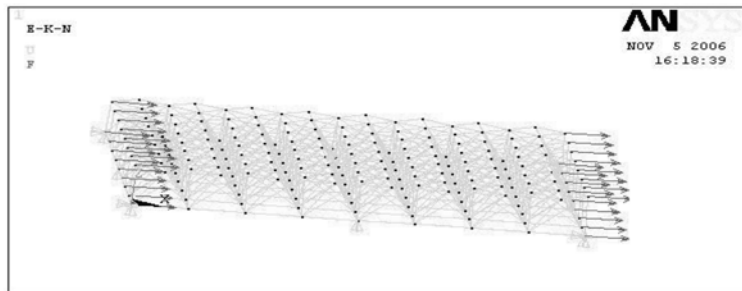
Fig. 16 shows the finite element model of 8 m × 8 m grid, consisting of a total of 64 single tensegrity units, measuring 8 × 8 m in plan and 0.5 m in height. This is an extension of the model of 2 × 2 grid, which was validated experimentally. All the member lengths, properties and boundary conditions were considered the same as for the 2 × 2 grid. The structure was thus supported on the four corner nodes only. It should be noted that the rigidity ratio (see Eq. 1) for this system was 52.74. For the purpose of analysis, a dead load of 200 N/m² from sheeting was considered in addition to the self weight of the members. The intensity of the imposed load was considered as 750 N/m² (for inaccessible roofs) as per IS 875 II (1987). Wind loads were determined for Delhi region as per IS 875 III (1987), for which a basic wind speed of 47 m/s is prescribed, resulting in a design wind pressure, $p_z = 891.2$ N/m². Wind force was determined using

$$F = (C_{pe} - C_{pi})Ap_z \quad (8)$$

where C_{pe} and C_{pi} respectively denote the external and the internal wind pressure coefficients, A the area



(a)



(b)

Fig. 16 Finite element model of 8×8 tensegrity grid structure (a) Perspective view, (b) Top view

of the surface considered and p_z the design wind pressure. C_{pi} was considered as ± 0.7 appropriate considering large permeability. For wind force acting normal to the roof, $C_{pe} = -0.8$ and $C_{pi} = +0.7$ (pressure from inside) offered the worst combination. All the loads were distributed among the various nodes in proportion to their tributary area.

Analysis of the 8×8 grid structure for these loads showed that although all member forces were within the safe limits, and few cables underwent stress reversal under the combination (Dead loads + Wind loads). The overall structure was safe from strength considerations, taking into account the redundancy of the structure. However, a maximum deflection in excess of span/ 325 was observed in the central node for the combination (Dead loads + Imposed loads). Hence, the structural system warranted modification. After a number of trials, a combination of following steps resulted in the compliance with both strength and serviceability criteria: (a) provision of additional vertical supports at 4 m spacing on the periphery (b) increasing the height of the structure from 0.5 m to 0.8 m. (c) increasing the cable area such that the rigidity ratio for this system reduced from 52.74 to 10. With these changes, the load capacity of the cable increased to 20.96 kN. The joint strength remained unaltered. Analysis of the

modified structural system revealed that the maximum deflection of the bottom central node reduced to 14 mm, much below the limit prescribed from the point of view of serviceability. Maximum cable force was found to be 3.5 kN and the maximum strut force 6 kN, which are within the safe limits. Again, few cables were rendered slack, however, without affecting the overall safety of the structure due to the inherent redundancy. Thus, the proposed 8×8 grid structure is suitable for field applications requiring about 8 m span.

6. Conclusions

This paper has explored the possibility of employing a new type of tensegrity grid structure as an alternative roof structure. The proposed grid was achieved by joining the individual half-cuboctahedron tensegrity elements. The resulting grid is a single cohesive unit, connected at the common cables, rather than nodes, as in the case of previously reported structures. In addition, the present method reduces the number of cables. The system has an opening/ closing mechanism which imparts it the flexibility of quick erection when required and packaging the entire structure after the intended use. The proposed grid systems are therefore suitable for temporary shelters, such as in the calamity effected areas. Being light-weight and compact, they can be transported easily and erected within short notice. They can also be employed for providing roof structures in fairs, expositions and industrial sheds.

The paper also covered the fabrication, instrumentation, and destructive testing of two structures- a single half-cuboctahedron module and a 2×2 prototype tensegrity grid. The structures were continuously monitored using strain gauges bonded on the members and LVDTs installed below key joints. Failure pattern and measurements showed that the actual end conditions of the strut with the present system of joints are that of partial fixity, and hence an effective length coefficient of 0.7 is appropriate for design.

Finite element models of the structures were developed and updated based on the experimental observations and produced structural response matching well with experiment, in terms of both the member forces as well as the joint deflections. The condition of fixing the bottom nodes against both horizontal and vertical deflections is found to match closer with the observed structural behaviour. The finite element model was extended to 8×8 tensegrity grids, the analysis of which revealed that it is feasible to extend the proposed system to spans as large as 8m. Both the strength and serviceability criteria were found to be satisfied by providing four additional supports along the periphery, increasing the structure's height to 0.8 m and the rigidity ratio to 10. The strength of the joint governs the design from strength point of view. Presently, the joint is considered at conceptual level only. Experimental studies are currently underway to design the joint more rigorously and enhance its load capacity.

In conclusion, the proposed dismountable tensegrity grid is easy to fabricate, assemble and dismantle and there is no necessity of lifting machines or skilled labour for field deployment. The structure requires less space for storage and is easy to transport. Hence, they have great potential for providing light-weight roof systems for the modern structures. Future studies aim at combining the proposed grid with tensegrity based columns so as to result in a complete tensegrity based structural solution.

References

- ANSYS version 9 (2004).
Argyris, J.H. and Scharpf, D.W. (1972), "Large deflection analysis of prestressed networks", *Journal of the*

- Structural Division*, ASCE, **98**, 633-54.
- Batten, M., Boorman, R. and Leiper, Q. (1999), "Use of vibrating wire strain gauges to measure loads in tubular steel props supporting deep retaining walls", *Proc. of Institution of Civil Engineers, Geotechnical Engineering*, **137**, 3-12.
- Fest, E., Shea, K. and Smith, I.F.C. (2004), "Active tensegrity structure", *J. Struct. Eng.*, ASCE, **130**, 1454-65.
- Fu, F. (2005), "Structural behavior and design methods of tensegrity domes", *J. Constr. Steel Res.*, **61**, 23-35.
- Fuller, R.B. (1962), *Tensile integrity structures*, United States Patent No. 3, 063, 521.
- Gantes, C. (1997), "An improved analytical model for the prediction of the nonlinear behavior of flat and curved deployable space frames", *J. Constr. Steel Res.*, **44**, 129-158.
- Hanaor, A. (1993), "Double layer tensegrity grids as deployable structures", *Int. J. Space Struct.*, **8**, 135-43.
- IS: 800 (1984), *Code of practice for general construction in steel*, Bureau of Indian Standards.
- IS: 875 II (1987), *Code of practice for design loads (other than earthquake) for buildings and structures: Part II Imposed loads*, Bureau of Indian Standards.
- IS: 875 III (1987), *Code of practice for design loads (other than earthquake) for buildings and structures: Part III Wind loads*, Bureau of Indian Standards.
- IS: 1239 I (1990), *Mild Steel Tubes, Tubulars and Other Wrought Steel Fittings - Specification - Part 1: Mild Steel Tubes*, Bureau of Indian Standards.
- IS: 1835 (1976), *Specification for Round Steel Wire for Ropes*, Bureau of Indian Standards.
- IS: 3459 (1977), *Specification for Small Wire Ropes*, Bureau of Indian Standards.
- Kebiche, K., Kazi-Aoual, M.N. and Motro, R. (1999), "Geometric non-linear analysis of tensegrity systems", *Eng. Struct.*, **21**, 864-76.
- Panigrahi, R. (2007), "Development, analysis and monitoring of dismountable tensegrity structure", Ph. D. thesis, Department of Civil Engineering, Indian Institute of Technology Delhi.
- Quirant, J., Kazi-Aoual, M.N. and Motro, R. (2003), "Designing tensegrity systems: the case of a double layer grid", *Eng. Struct.*, **25**, 1121-30.
- Snelson, K. (2004), <http://www.kennethsnelson.net/> accessed January 2005-December 2005.
- Stern, I.P. (1999), "Development of design equations for self deployable N- strut tensegrity systems", M.S. Thesis, University of Florida.
- Sultan, C. and Skelton, R.E. (2003), "Deployment of tensegrity structures", *Int. J. Solids Struct.*, **40**, 4637-57.
- Tokyo Sokki Kenkyujo Company Limited (TML). (2006), <http://www.tml.jp/e/>.
- Tibert, A.G. and Pellegrino, S. (2002), "Deployable tensegrity reflectors for small satellites", *J. Spacecraft Rockets*, **39**, 701-09.
- Tibert, A.G. and Pellegrino, S. (2003), "Deployable tensegrity masts", *Proc. of 44th AIAA/ASME/ASC/ASCE/AHS/ASC Structures Structural Dynamics and Materials Conf. and Exhibit*, Norfolk 1-11.
- Vu, K.K., Liew, J.Y.R. and Krishnapillai, A. (2005), "Deployable tension strut structure: conceptualization to implementation", *J. Constr. Steel Res.*, **62**, 195-206.
- Vu, K.K., Liew, J.Y.R. and Krishnapillai, A. (2006), "Rapidly deployed tension-strut structures", *Proc. of 8th Int. Conf. on Steel, Space and Composite structures*, 15-17 May, Kuala Lumpur, 145-52.
- Wang, B.B. and Li, Y.Y. (2003), "Novel cable strut grids made of prisms: part I Basic theory and design", *Int. J. Space Struct.*, **44**, 93-125.
- You, Z. and Pellegrino, S. (1997), "Cable-stiffened pantographic deployable structures 2. mesh reflector", *AIAA J.*, **35**, 1348-55.
- Zhang, J.Y. and Ohsaki, M. (2006), "Adaptive force density method for form-finding problem of tensegrity structure", *Int. J. Solids Struct.*, **43**, 5658-73.